



Optical Bloch oscillation and resonant Zener tunneling in one-dimensional quasi-period structures containing single negative materials

Xiubao Kang, Zhiguo Wang*

Pohl Institute of Solid State Physics, Tongji University, Shanghai 200092, PR China

ARTICLE INFO

Article history:

Received 5 June 2008

Received in revised form 27 September 2008

Accepted 10 October 2008

PACS:

42.15.Dp

71.20.-b

42.25.Hz

78.67.Pt

ABSTRACT

We studied the optical Bloch oscillation and resonant Zener tunneling in macroscopic quasi-period structures of alternatively stratified single negative and dielectric slabs. By a decrease in the thicknesses of the dielectric slabs, the electronic potential of crystals subjected to external dc electric fields is mimicked and the optical Wannier–Stark ladder (WSL) is realized. Both scattering states and the time-resolved transmission of a short pulse are provided to show the existence of the optical analogue of electronic Bloch oscillation. At a critical gradient, the resonant photon Zener tunneling is demonstrated both from the amplitude and the time delay in the transmitted signal of a short pulse.

© 2008 Elsevier B.V. All rights reserved.

1. Introduction

Electron Bloch oscillation [1] and resonant Zener tunneling [2] are well developed concepts describing the behaviors of electrons in crystals subjected to external dc electric fields. The former one describes the oscillations of electrons both in real and k-space, and quantization of this quasi-classical motion engenders Wannier–Stark ladders (WSLs) [3] which contains some localized equi-distance energy states. For the cases of weak external field, WSLs belonging to different energy band are separated by band gaps. The electron Bloch oscillation come into force as the electrons accelerated by the external force inside the energy band and reflected by the band gaps at the edges. With the increasing of external electric fields, the anticrossing of those neighboring bands occurs and the gap between lower WSL and the higher one disappears. Rather than be reflected at the band edge, electrons will tunnel to the higher band without additional energy, and thus the resonant Zener tunneling appears. Although the concept of Bloch oscillation has been predicted as long as the beginning of the last century, the observation of this fascinating phenomenon is not easy. The main reason that accounts for the difficulties in the observation is that the dephasing time of electrons in crystals is shorter than the oscillation period h/eEd , where d is the lattice period, E is the external electric field, e is the electron charge and h is the Plank constant. By the dephasing time, the effects of electron–

phonons scattering and Zener tunneling which make electrons lose their continuity in the phase is addressed. The advent of the high-purity semiconductor superlattices (SSL) shed some lights on the observation of electron Bloch oscillation [4] for that the oscillation periods in these system is much faster owing to bigger super-cells [5]. Time-resolved Bloch oscillations were then indeed observed in SSL system [6–9].

Photons have the similar nature of wave with electrons but they are not charged. Some quantum properties of electrons can be realized in the photons without the tanglement of phonon scattering. Optical Bloch oscillation or Zener tunneling have been predicted and observed in various structures in recent years [10–23]. Those structures include: linearly chirped Moiré grating written in the core of an optical fiber [11,12], unchirped Bragg grating comprising high and low index layers superimposed with a linearly variation of refractive index or thicknesses [10,14–16], exponentially chirped Bragg gratings [17], unchirped Bragg gratings with a slowly varying lateral confinement [18,19] and waveguide arrays [20–23]. These realized structures are either intrinsically two-dimensional (2D) or made of electrochemical etched porous silicon in nm range.

The experimental realization of the metamaterials [24] has evoked special interests in many applications of their novel properties. Theoretical work of realizing optical Bloch oscillation in structures involving metamaterials has been presented recently [25]. Here we demonstrate the existence of microwave optical Bloch oscillation and resonant photonic Zener tunneling in one-dimensional (1D) macroscopic structures with the help of single

* Corresponding author.

E-mail address: zgwang@mail.tongji.edu.cn (Z. Wang).

negative materials (SNG) [26,27]. The concept of SNG depicts one kind of materials with one of their two fundamental electromagnetic parameters, permittivity or permeability, being negative and the other one being positive. Propagating waves in conventional materials with both permittivity and permeability being positive turn to evanescent fields inside bulk SNG and can not transmit in such materials, which make bulk SNG perfect reflectors. A conventional dielectric layer sandwiched between two SNG layers can form a Fabry–Perot resonator with the resonant frequency adjustable by simply changing the thicknesses of the dielectric layer.

In the typical realizations of electron Bloch oscillation in SSL such as in Ref. [6], a sequence of quantum wells subjected to dc electric field was used. The application of the external field leads to gradual localization of wave functions along the direction of external electric force, and electrons will oscillate among those localized states. As photons can not be accelerated as electrons do under the effects of dc electric field, micro-cavities array with properly modulated resonant frequencies are the best analogue to the quantum wells array subjected to dc electric field [16]. Optical Bloch oscillation and resonant Zener tunneling should be observable in a sequence of Fabry–Perot cavities composed by a series dielectric layers sandwiched between SNG layers.

The structures considered in this paper are composed by alternately stratified dielectric and SNG layers whose permeability is negative (MNG). As shown in Fig. 1, the whole structure is $AB_1A-B_2\dots AB_nAB_{n+1}A\dots B_9A$. The layer of B_n is the n th dielectric layer with a thickness d_n and all A layers are composed by MNG with a thickness of $d_a = 6$ mm. The unit of the structures is a micro-cavity of AB_nA . All electromagnetic waves considered in this paper impinge from the left-side of the structure and transmit along the direction from B_1 to B_9 . The corresponding parameters of the MNG layers are [26]:

$$\varepsilon_{\text{MNG}} = 2\varepsilon_0, \quad \mu_{\text{MNG}} = \left(1 - \frac{\beta}{f^2}\right)\mu_0, \quad (1)$$

where $\beta = 100$ and f is the frequency of the incident electromagnetic wave measured in GHz. The parameters of B_n layers are $\varepsilon_1 = 2\varepsilon_0$, $\mu_1 = \mu_0$. As all the layers, SNG or conventional materials can be simulated by the composite right/left-hand transmission line (CRTL) with very low loss [27], we neglected the loss in the following calculations. Comparing with the metal which has negative permittivity in microwave frequency, SNG with either negative permittivity

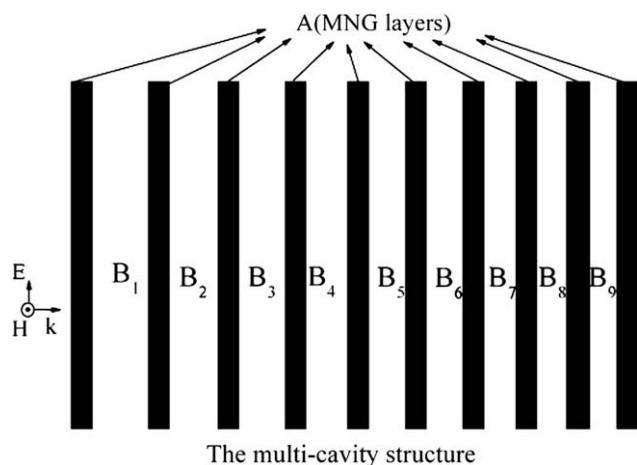


Fig. 1. The typical structure. The black layers denote MNG layer and the enclosed white layers are of dielectric. There's a gradient in the inverse of the dielectric layer thickness. Electromagnetic waves impinge from the left side of the structure normally.

or negative permeability can be realized in the CRTL mode. Furthermore, both the effective permeability and permittivity of each kind of SNG are adjustable in a large range. Similar to cavities composed by dielectric layers sandwiched by Bragg mirrors, the frequency of fundamental cavity modes in such SNG involved cavities should be approximately linearly related to the inverse of the cavity thickness. When a gradient $\delta \frac{1}{d_1}$ in the inverse of layer thicknesses of neighboring dielectric is introduced as

$$\frac{1}{d_{n+1}} - \frac{1}{d_n} = \delta \frac{1}{d_1} \quad (2)$$

there should be a micro-cavities series with an equal interval between the resonant frequencies of neighboring micro-cavities. The thickness of the first dielectric layer is chosen as $d_1 = 15$ mm. Although many factors such as the existence of the neighboring micro-cavities, the boundaries of the whole structure, the dispersion of the SNG and the frequency dependent optical length of the SNG layer may all slightly affect the resonant frequency of each micro-cavity, the intervals between resonant frequencies of neighboring micro-cavities can still approximately be seen as equal and the expected phenomena should be observable.

For electrons in crystals subjected to dc electric field, flat energy bands composed by delocalized state of Bloch waves are suppressed and tilted by the external field and localized WSLs appear. Arising from the twofold interplay of periodic structure and the external field, electrons Bloch oscillation among a WSL will take place. We firstly demonstrate an optical analogue of WSL in the structure. In Fig. 2a, we present the scattering states map [16] calculated by transfer matrix methods (TMM) [28] inside periodic structure ($\delta = 0$). The scattering states map provides the electric field intensity of each position inside the structure when plane EM waves of unit amplitude impinge onto the structure normally. The field distribution is represented by the brightness. The periodic structure is schematically shown by the square-lattice below the map. It can be clearly found that there's no field localization among different cavities in the periodic structures. Composed by some delocalized states in space, each bright band is the optical analogue to an electronic energy band of a periodic potential. The logarithm of transmission of the structure is illustrated in Fig. 2b. Fig. 2c shows the scattering states map of a structure with $\delta = 0.12$. One can find that the energy bands of the structure take critical change. Comparing with Fig. 2a and c demonstrates a sequence of strongly localized states which compose a tilted energy band and is clearly an optical counterpart of electron WSL. In the corresponding transmission spectrums shown in Fig. 2d ($\delta = 0.12$), the WSL is characterized by equi-distance peaks generated from those localized states. The lowermost localized state in Fig. 2c and d belongs to another WSL.

It can be seen from Fig. 2d that the whole transmission spectrums are just very similar to those of much complicated structures in the former papers of the WSL [10–19]: (i) the transmission peaks near the center part of the energy band are approximately equidistant (here, $\Delta f \approx 0.289$ GHz); and (ii) the frequency distances between those outer peaks get obviously wider than those between central peaks. However, the inequality of the frequency distances is not consistent with the classic theory of WSL. The advent of the two boundaries of the whole structure which violates the periodic boundary condition that is necessary for the classical theory of Bloch oscillation may account mainly for this inequality. As one can find in Fig. 2c, the peaks lying at the edge of the band are originated from the resonant mode of the micro-cavities near the boundaries of the structure. It's not surprise that the resonant frequencies of these micro-cavities will deviate farther from the predicted ones.

To demonstrate the optical counterpart of Bloch oscillation, we calculated the propagation of a 2 ns length pulse inside the

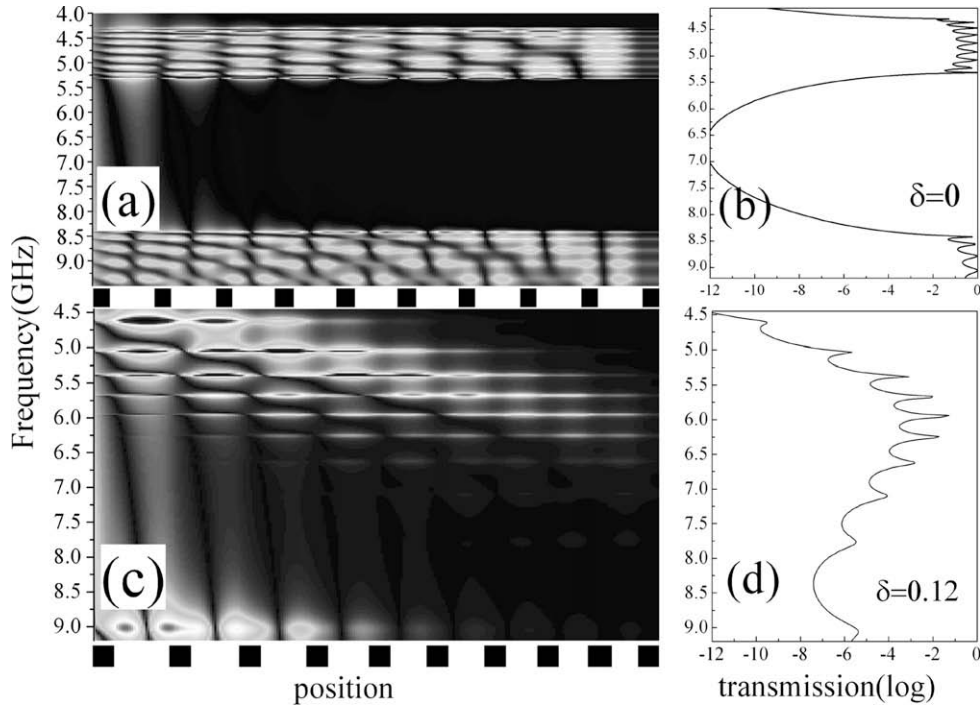


Fig. 2. Scattering states maps for structures (a) without gradient $\delta = 0$ or (c) with a gradient of $\delta = 0.12$. The brightness shows the intensity of the electric field. The square lattice below (a) or (c) shows schematically the structure: the black layers are SNG, and the white ones are dielectric layers. (b) and (d) are the corresponding transmission for the structure left to it.

structure with $\delta = 0.12$. The pulse which is chosen to be localized at the fifth peak ($f = 5.95$ GHz) and covers the central three peaks of the tilted transmission band impinges from the left side of the structure at the time $t = 0$. In frequency domain the pulse is depicted by $g(f)$

$$g(f) = \frac{1}{\pi\Delta f} \exp\left[-\frac{1}{2}\left(\frac{f-f_0}{\Delta f}\right)^2\right] \quad (3)$$

which is shown in Fig. 3 by a dashed orange line (gray, if the figure is black and white in print). The solid black line in Fig. 3 is the transmission spectrum of the structure $\delta = 0.12$. The reason we choose the pulse in the central of the WSL is that, as the resonant peaks lying at the center of the WSL are arisen from the central micro-cavities of the structure, the transmission of this pulse inside the structure will be less affected by the boundaries of the whole structure. Thus the physical essential of the WSL and optical Bloch oscillation will be not be covered up by the effects deriving from the finiteness of the whole structure.

By the scattering state method [29], the temporal and coordinate-dependent electric field distribution within structures can be found as

$$E(z, t) = \frac{1}{2\pi} \int_{-\infty}^{+\infty} E(f, z)g(f) \exp(-i2\pi ft)df, \quad (4)$$

where z is the coordinate in the transmission direction, $E(f, z)$ is the scattering states calculated from TMM. The oscillation of a particle can be demonstrated both in position and in time domain by the scattering state of the short pulse. The results are shown in Fig. 4.

One can find from Fig. 4a that most energy of the pulse is reflected at the left boundary of the structure and small percentage impinges into the structure. Inside the structure, the latter part exhibits a clear oscillation which is just the optical counterpart of electronic Bloch oscillation in crystals subjected to dc electric fields. Some percentage of the pulse leaks out of the structure when the pulse reaches the boundaries. As shown in Fig. 4b, the

leakage from the right side of the structure can be calculated as the time-resolved transmission:

$$T(t) = \frac{1}{2\pi} \int_{-\infty}^{+\infty} g(f)a(f) \exp(-i2\pi ft)df, \quad (5)$$

where T is transmitted electric signal as function of time, and $a(f)$ is the transmission coefficient for the frequency f . The period of time domain optical Bloch oscillation can be measured as the interval between the neighboring transmission peaks (3.45 ns for this gradient). Unlike in those Refs. [14–16] about optical Bloch oscillation

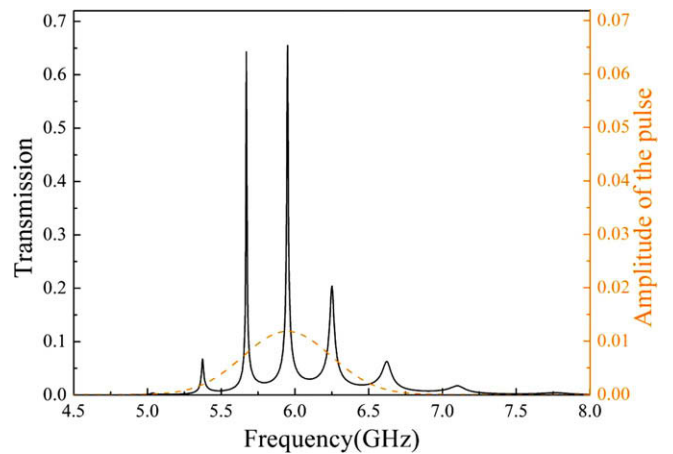


Fig. 3. The WSL and the frequency distribution of the incident pulse employed in the demonstration of Bloch oscillations. The solid black line is the transmission spectrum of the tilted structure with a gradient of $\delta = 0.12$. The WSL is clearly seen as a sequence of equi-distance transmission peaks which has also been shown in Fig. 2d in a different manner. The dashed orange (gray, if the figure is black and white in print) line shows frequency distribution of the pulse. (For interpretation of the references in colour in this figure legend, the reader is referred to the web version of this article.)

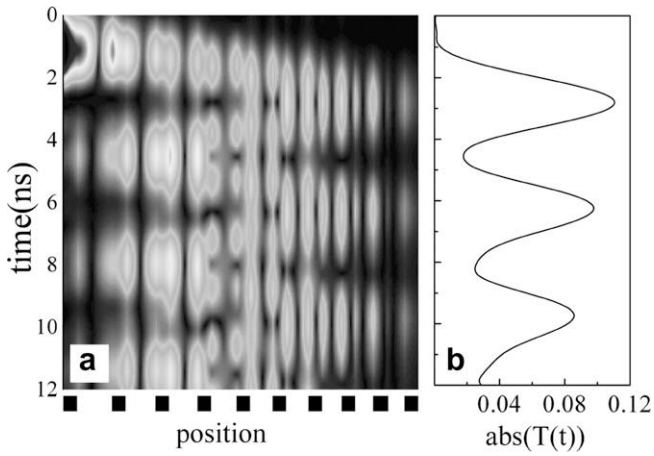


Fig. 4. The optical Bloch oscillation: (a) The trace of a pulse which is centered at the fifth peak of the first WSL of the structure with $\delta = 0.12$; (b) the amplitude of transmitted signal as a function of time. The structure is shown in the lower part of (a) where the black lattices denote the SNG layers. The pulse impinges onto the structure from left.

in one-dimensional structures where the oscillation period is of ps scale, the periods of the Bloch oscillation in our structures are of ns scale. According to the correspondence principle, the oscillation period τ should be inversely proportional to the energy difference between the neighboring localized states in the WSL, that is, $\tau = h/\Delta E$. For the gradient $\delta = 0.12$, the energy difference between neighboring localized states is $\Delta E = 1.2 \mu\text{eV}$ (corresponding to $\Delta f = 0.289 \text{ GHz}$), and the temporal interval is thus $\tau = 3.46 \text{ ns}$, which is in good agreement with interval 3.45 ns.

In the electronic case the external field and the period of the oscillation should be inversely related ($\tau = h/eEd$), that is, the larger the external dc electric field the shorter the Bloch oscillation will be. In Fig. 5a, we give the temporal responses of the Gauss pulses transmitted from structures with different δ s. The pulse illuminated to each structure is centered at the fifth peak of the WSL of corresponding structure and covering the neighboring fourth and sixth peaks. One can clearly see that the temporal intervals between transmission peaks is equal to each other for each gradient and the temporal intervals decrease as the gradient δ increases. In Fig. 5b, we figure out the relation between temporal interval τ and gradient δ . The results indeed show the expected tendency.

In the structures considered here, clear demonstrations of the optical counterpart of electronic resonant Zener tunneling are also available. For the occurrence of the electronic resonant Zener tunneling, there firstly should be the disappearance of the energy gap between two adjacent WSLs. A WSL is extended by the dc field in the frequency domain and one of its edges will ramp to a neighboring WSL when the external field is strong enough, and thus the gap disappears. Before discussing the optical counterpart of resonant Zener tunneling, we will firstly demonstrate the process of the combination of the neighboring WSL. In Fig. 6, the peak labeled as **a** is the last transmission peak in the lower WSL and the peak labeled as **b** is the first transmission peak in the neighboring higher WSL. The locations of the two peaks representing the one edge of the corresponding WSL. As the δ increases, the evolutions of these two peaks are shown in Fig. 6. From Fig. 6a to c, the gradient of the structure are $\delta = 0.15, 0.18,$ and 0.22 , respectively. The peaks lying at the left side of peak **a** in Fig. 6b and c are the inner peaks of the first WSL. One can find that the upper edge of the first WSL extends to higher frequency direction as δ increases, while the lower edge of the second WSL keeps almost unchanged during this process. Transmission peaks representing two localized resonant states belonging to different WSLs began to couple with each other when

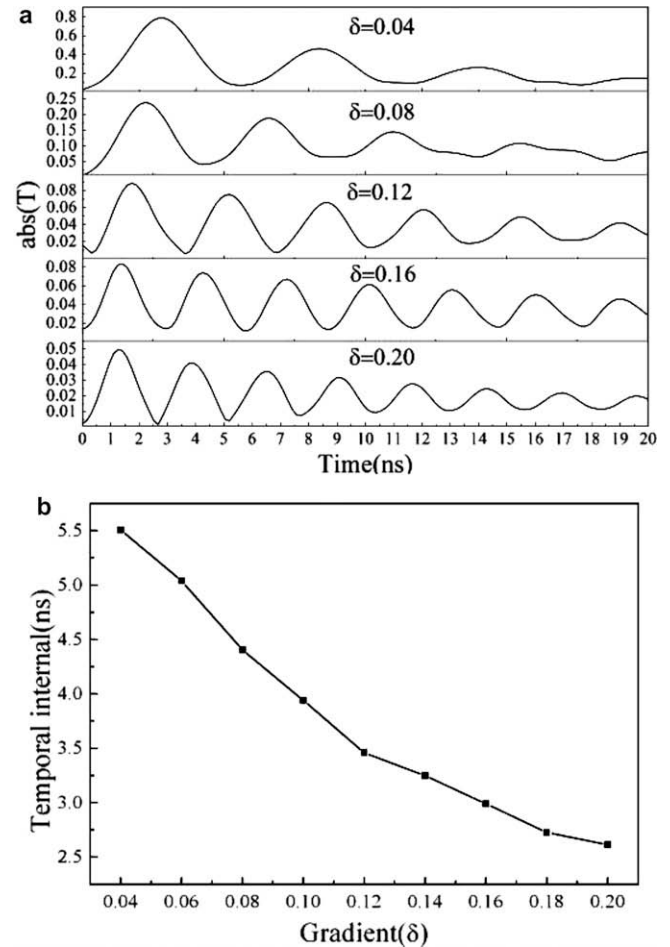


Fig. 5. (a) Temporal response of pulses located at the fifth transmission peak of corresponding WSLs. The δ is labeled in the center of each panel. A decrease of time interval as the gradient increases is directly demonstrated; and (b) temporal interval as a function of δ .

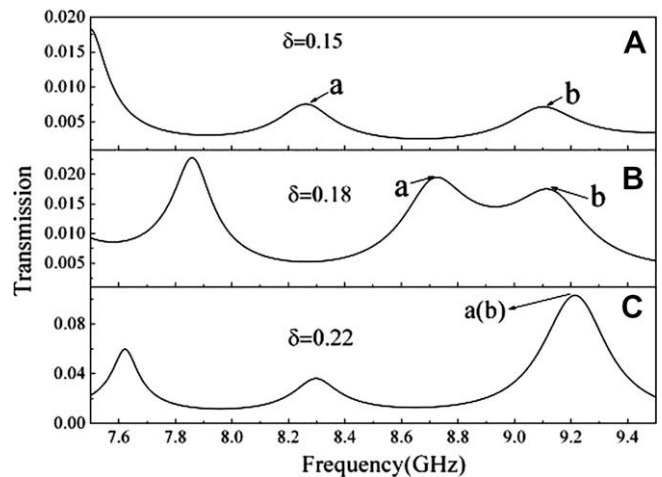


Fig. 6. Couplings of neighboring WSLs. From upper to below the value of δ are 0.15 (a), 0.18 (b), 0.22 (c). As the gradient increases the peak **b** denoting the low frequency band edges of the second WSL keeps almost unchanged, while the peak **a** which is the high frequency band edge of the first WSL ramps towards higher frequency. Neighboring WSL began to overlap with each other obviously when $\delta = 0.18$. As δ reaches 0.22 the last transmission peak **a** of the first WSL covers the first transmission peak **b** of the second WSL completely. The peaks lying left to the peak **a** peaks belonging to the lower WSL.

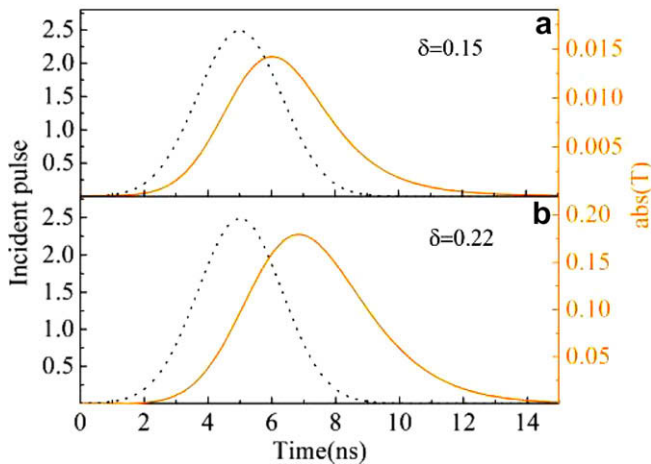


Fig. 7. Time responses of pulses centered at the first peak of the second WSL for two structures: (a) $\delta = 0.15$ and (b) $\delta = 0.22$. The dotted line is the incident pulse. In the frequency domain, each incident pulse is designed to cover the first peak of the second WSL wholly. The transmitted signal for the gradient $\delta = 0.22$ exhibits a longer time delay and larger amplitude. (For interpretation of the references in colour in this figure legend, the reader is referred to the web version of this article.)

the frequency difference between them is smaller than the width of the peaks: obvious overlap can be found when $\delta = 0.18$ (Fig. 6b). As δ reach 0.22, these two neighboring resonant states cover up with each other and the merged peak get enhanced greatly (Fig. 6c). Thus, the neighboring WSLs combine with each other completely. By the transmission amplitude, it is firstly characterized by larger amplitude which is as large as two times the sum of both single peaks for smaller gradient ($\delta = 0.18$). Besides the enlargement in the amplitude, the merged transmission peak also gets broader, which is the result of the repulsion between these two coupled resonant states [16].

Driven by a strong external dc electric field, an electron lying in one WSL can tunnel to states belonging to another one when two neighboring WSLs merge with each other in the process of Zener tunneling. The electron experiences resonant states belonging to different WSLs. To observe the optical counterpart of the Zener tunneling, we calculated the time-resolved transmission of two specially chosen pulses through two different structures with the corresponding gradient being 0.15 for Fig. 7a and 0.22 for Fig. 7b. The incident Gauss pulses are centered at the first transmission peak of the second WSL of the corresponding structure and covering the single transmission peak. The two pulses are almost centered at the same frequency because the lower band edge keeps almost unchanged during the increase process of δ . The temporal domain profile of the incident pulse is illustrated as the black dotted line in corresponding figure. The transmission signals of both cases are illustrated by solid orange (gray, if the figure is black and white in print) lines in corresponding figures. As the frequency range of the pulse is covering only one resonant frequency, there are no oscillations for both pulses, which are different from Fig. 4. For the occurrence of an oscillation the pulse should cover at least two resonant frequencies [30]. For the case shown in Fig. 7b, the incident pulse is centered simultaneously at the frequency of the first energy level of the higher WSL and the last energy level of the lower WSL. Comparing with Fig. 7a, there's a longer time delay in the transmitted signal in Fig. 7b, which should be attributed to the establishment of the double resonances [14].

Before leaking out of the structure, the pulse experiences double resonances one of which belongs to the first WSL and the other belongs to the second one. Similar to the electronic case the double resonances of a single pulse can be a direct manifestation of the occurrence of the resonant Zener tunneling. As a result of the coupling between the two micro-cavities, the amplitude of the transmitted signal in Fig. 7b is almost ten times as large as that from structure where no tunneling occurs in Fig. 7a, which can be referred as another character of the occurrence of the resonant Zener tunneling.

In conclusion, we have studied the transmittances of a kind of simple 1D quasi-periodic structures involving SNG layers. The optical analogue of fundamental electronic concepts of Wannier–Stark ladder, Bloch oscillation and resonant Zener tunneling are demonstrated by scattering states maps and time-resolved transmissions in microwave range. All the results should be realizable in macroscopic structures in composite right/left-hand transmission lines.

Acknowledgments

We thank Hong Chen for valuable discussions. This work was supported by National Basic Research Program (973) of China under Grant No. 2006CB921701, National Natural Science Foundation of China under Grant No. 10634050, and Shanghai Science and Technology Committee.

References

- [1] F. Bloch, Z. Phys. 52 (1928) 555.
- [2] C. Zener, Proc. R. Soc. London A 145 (1934) 532.
- [3] G.H. Wannier, Phys. Rev. 117 (1960) 432; G.H. Wannier, Rev. Mod. Phys. 34 (1962) 645.
- [4] L. Esaki, R. Tsu, IBM J. Res. Dev. 14 (1970) 61.
- [5] J. Bleuse, G. Bastard, P. Voisin, Phys. Rev. Lett. 60 (1988) 220.
- [6] E.E. Mendez, F. Agulló-Rueda, J.M. Hong, Phys. Rev. Lett. 60 (1988) 2426.
- [7] K. Leo, P.H. Bolivar, F. Brüggemann, R. Schwedler, K. Köhler, Solid State Commun. 84 (1992) 943.
- [8] C. Waschke, H.G. Roskos, R. Schwedler, K. Leo, H. Kurz, K. Köhler, Phys. Rev. Lett. 70 (1993) 3319.
- [9] J. Feldmann, K. Leo, J. Shah, D.A.B. Miller, J.E. Cunningham, Phys. Rev. B 46 (1992) R7252.
- [10] G. Monsivais, M. del Castillo-Mussot, F. Claro, Phys. Rev. Lett. 64 (1990) 1433.
- [11] C.M. de Sterke, J.N. Bright, Peter A. Krug, T.E. Hammon, Phys. Rev. E 57 (1998) 2365.
- [12] I. Talanina, C.M. de Sterke, Phys. Rev. A 63 (2001) 053802.
- [13] G. Lenz, I. Talanina, C. Martijn de Sterke, Phys. Rev. Lett. 83 (1999) 963.
- [14] R. Sapienza, P. Costantino, D. Wiersma, M. Ghulinyan, C.J. Oton, L. Pavesi, Phys. Rev. Lett. 91 (2003) 263902.
- [15] V. Agarwal, J.A. del Río, G. Malpuech, M. Zamfirescu, A. Kavokin, D. Coquillat, D. Scalbert, M. Vladimirova, B. Gil, Phys. Rev. Lett. 92 (2004) 097401.
- [16] M. Ghulinyan, C.J. Oton, Z. Gaburro, L. Pavesi, C. Toninelli, D.S. Wiersma, Phys. Rev. Lett. 94 (2005) 127401.
- [17] P.B. Wilkinson, Phys. Rev. E 65 (2002) 056616.
- [18] A. Kavokin, G. Malpuech, A.D. Carlo, P. Lugli, F. Rossi, Phys. Rev. B 61 (2000) 4413.
- [19] G. Maluech, A. Kavolin, G. Panzarini, A. Di Carlo, Phys. Rev. B 63 (2001) 035108.
- [20] U. Peschel, T. Pertsch, F. Lederer, Opt. Lett. 23 (1998) 1701.
- [21] H. Trompeter, T. Pertsch, F. Lederer, D. Michaelis, U. Streppel, A. Bräuer, Phys. Rev. Lett. 96 (2006) 023901.
- [22] W. Lin, X. Zhou, G.P. Wang, C.T. Chan, Appl. Phys. Lett. 91 (2007) 243113.
- [23] W. Lin, G.P. Wang, Appl. Phys. Lett. 91 (2007) 143121.
- [24] D.R. Smith, W.J. Padilla, D.C. Vier, S.C. Nemat-Nasser, S. Schultz, Phys. Rev. Lett. 84 (2000) 4184.
- [25] A.R. Davoyan, I.V. Shadrivov, A.A. Sukhorukov, Y.S. Kivshar, Opt. Express 16 (2008) 3299.
- [26] H. Jiang, H. Chen, H. Li, Y. Zhang, S. Zhu, Appl. Phys. Lett. 83 (2003) 5386.
- [27] L. Zhang, Y. Zhang, L. He, H. Li, H. Chen, Phys. Rev. E 74 (2006) 056615.
- [28] J.B. Pendry, Adv. Phys. 43 (1994) 461; P. Yeh, A. Yariv, C. Hong, J. Opt. Soc. Am. 67 (1977) 423.
- [29] G. Malpuech, A. Kavokin, Semicond. Sci. Technol. 16 (2001) R1.
- [30] K. Leo, J. Shah, E.O. Göbel, T.C. Damen, S. Schmitt-Rink, W. Schäfer, K. Köhler, Phys. Rev. Lett. 66 (1991) 201.